Multi-rate operational space control of compliant motion in robotic manipulators

Ngoc Dung, Vuong
Marcelo H. Ang, Jr.
Mechanical Department
National University of Singapore
Singapore
{ndvuong, mpeangh}@nus.edu.sg

Tao Ming, Lim
Ser Yong, Lim
Singapore Institute of Manufacturing Technology
Singapore
{tmlim, sylim}@SIMTech.a-star.edu.sg

Abstract— **In this paper, we introduce a new multi-rate hybrid motion and force control using operational space framework. Conventional implementation of operational space control (OSC) does not perform well in the presence of model uncertainties. In order to overcome this issue, a two layered hierarchical controller structure is proposed in this paper. In the outer control loop, the control torque from the OSC is applied to the joint space dynamic model of the robot. By integrating the output of this system, reference joint velocities for the next control loop can be obtained. At the inner control loop, the conventional computed-torque control scheme is used to ensure the robot can track the above desired joint velocities. To illustrate the effectiveness of the proposed controller, intensive experiments have been conducted on the Mitsubishi PA10 7-DOF manipulator. Experimental results indicate that there is a significant improvement in comparison to the conventional implementation and the proposed approach is shown to have performed favorably in comparison to the commercial force controller from PushCorp.**

Keywords—**operational space control, hierarchical control, model-based control, force control.**

I. INTRODUCTION

Hybrid motion and force control capability is an essential requirement for interaction tasks. Although this capability has been realized by many researchers using laboratory robots, there are limited applications of these advanced control schemes on industrial manipulators. One possible explanation among others is that advanced control schemes require specialized knowledge about the robot such as the dynamic and joint friction models which are not always available.

Among motion and force control schemes for redundant manipulators, the operational space control framework, which was originally proposed in [1], is a prominent scheme because it dynamically decouples the operational (range) and null space. However, as pointed out in [2], the operational space framework, which works perfectly in the simulation environment, is sensitive to the accuracy of the robot model. This conclusion is further reinforced when we implemented the above OSC using the identified model as derived in [3] (this implementation is referred to as the conventional implementation of the OSC). Further investigation on the

robot model indicates that joint frictions at low-speeds are extremely complicated [4].

In order to see the effects of joint friction on the conventional OSC implementation, let's look at how torque control is implemented at each joint. For almost all industrial manipulators, the desired joint torque is achieved through controlling the motor current because of the lack of joint torque sensor. Figure 1 shows a typical control loop, $\tau_{desired}$ is the desired joint torque, $i_{desired}$ is the equivalent desired motor current, i is the motor current, τ_M is the actual torque provided by the motor, τ_L is the joint torque at the load side, n is the gear ratio, τ_{fric} is the friction torque and τ_{dist} is the unknown disturbance.

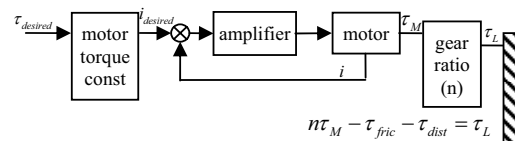$$n\tau_M - \tau_{fric} - \tau_{dist} = \tau_L$$

Figure 1. Typical joint torque control without torque sensor

Note that only current is controlled and it is assumed that torque control is achieved through the known motor torque constant. Frictions in the gear box and load side are not considered and need to be compensated by an outer loop. For the OSC framework, the outer feedback loop is closed via the task space variables (position and orientation) and contact force. In joint space control, the effects of the joint friction are collocated in the individual joint variables and thus easy to compensate by any joint space controllers. However, this is no longer true in task space control because the OSC has to indirectly compensate these effects through the kinematic chain. As a result, improper friction compensation in joint space degrades the task space tracking in motion control and causes the applied force to enter a limit cycle [5] (experimental result of this observation on the PA10 manipulator can be found in Section 3).

Although friction modeling is well documented in the literature, a perfect friction model which can capture all the

non-linear friction effects, especially frictions at the low-velocity region is still an open problem. At this region, friction is known to be highly nonlinear, with the hysteresis effect, Stribeck effect, position and/or time dependency and other nonlinearities. One of the most popular friction model that can be found in the literature is the LuGre friction model [5]. This model is known to capture most of the above effects except the position/time dependence effect. In order to cope with the position/time dependency, adaptive friction compensation is proposed in [6]. However, the implementation of these friction compensator schemes often requires good joint velocity estimation and/or reference joint velocities. From the practical point of view, these requirements are not easily fulfilled for the case where the motion and force are controlled in task space; thus, there are no explicit reference joint velocities. Moreover, the feedback joint velocities are normally obtained through numerical differentiation of the joint position measurements since most industrial robots do not have a joint velocity sensor. As a result, errors in the velocity estimation at low velocities will be magnified in the friction compensation due to velocity dependence of Stribeck and Coulomb friction models.

Another approach to compensate for the effects of joint friction in task space controller is to use a high frequency velocity feedback control loop at each joint. This approach will result in a so called inner-outer loop implementation [8, 9]. In this approach, the outer loop is closed in task space to generate the reference joint velocity using resolved motion rate control scheme. Subsequently, this reference joint velocity is passed to the inner loop which will compensate for the effects of joint friction and realize this reference velocity in a faster time scale compared with the outer loop. However, this control scheme does not take into account the system dynamics in the null space. Therefore, the task (range) space and null space cannot be dynamically decoupled.

In this paper, a new control structure is proposed where a higher-speed inner joint velocity control loop is used to reject the effects of local disturbances, whereas a lower-speed outer OSC loop is used to achieve motion and force tracking in task space and dynamically decouple the task and null space. In the outer control loop, the control torque from the OSC is applied to the joint space dynamic model of the robot. By integrating the output of this system, the reference joint velocities for the inner loop can be obtained. At the inner control loop, the reference joint velocities are realized by adopting the conventional computed-torque control scheme. The two main contributions of this paper are:

(i) a two layered hierarchical controller which takes into account the dynamic behaviors of the robot; and

(ii) a comprehensive experimental study is conducted to evaluate the effectiveness of the proposed control.

The rest of the paper is presented as follows: first, an overview on operation space control framework is presented. Subsequently, the proposed control scheme is detailed. Finally, the experimental results conducted on the PA10 manipulator is given to illustrate the effectiveness of the

proposed scheme and compared with current commercial force control solution.

II. THE OPERATIONAL SPACE CONTROLLER

A. Force-based operational space control

The main focus of operational space controllers (OSCs) for robot manipulators is to directly resolve the task space commands to joint torque commands without going through the inverse kinematic procedure. Two of the main concerns for the OSC approach for redundant robot manipulators lie in resolving the null-space and singularity issues. This paper only focuses on the implementation issues of the first problem which is theoretically addressed and solved in [1]. For the singularity issue, readers can refer to [10] for a comprehensive review as well as a robust singularity handling algorithm.

Assume that the joint space dynamic model of an n-DOF is:

$$A(q)\ddot{q} + C(\dot{q}, q) + g(q) + \tau_{Fric} + D_\tau = \tau - J^T F_{contact} \quad (1)$$

The equivalent task-space dynamics can be specified as:

$$\Lambda(x)\ddot{x} + \mu(x, x) + p(x) + D_F = F - F_{contact} \quad (2)$$

where $\{A, C, g, D_\tau\}, \{\Lambda, \mu, p, D_F\}$ are inertial matrix, Coriolis-Centrifugal, gravity and unknown disturbance in joint and task space accordingly:

$$\Lambda = \left(J A^{-1} J^T \right)^{-1} \quad (3)$$

$$\mu = \overline{J}^T C - \Lambda \dot{J} \dot{q} \quad (4)$$

$$p = \overline{J}^T g \quad (5)$$

$$D_F = \overline{J}^T D_\tau \quad (6)$$

$$\overline{J} = A^{-1} J^T \Lambda \quad (7)$$

The unified approach for motion and force control is then formulated as follows:

$$F = F_{motion} + F_{active-force} \quad (8)$$

where:

$$F_{motion} = \hat{\Lambda} \Omega u_{motion} + \hat{\mu} + \hat{p} \quad (9)$$

$$F_{active-force} = \hat{\Lambda} \overline{\Omega} u_{active-force} + F_{sensor} \quad (10)$$

$$u_{motion} = \ddot{X}_{de} + K_{md} \left(\dot{X}_{de} - \dot{X} \right) + K_{mp} \left(X_{de} - X \right) \quad (11)$$

$$u_{active-force} = K_{FP} \left(F_{desired} - F_{sensor} \right)$$
$$+ K_{FI} \int \left(F_{desired} - F_{sensor} \right) - K_{FV} \dot{X} \quad (12)$$

The generalized task specification matrices Ω and $\overline{\Omega}$ are pre-defined depending on the tasks. K_{md}, K_{mp} and K_{FI}, K_{FP}, K_{FV} are the gains for motion and force control

respectively. Noting that, equations (8-10) linearize the task-space dynamics of the robot (2); thus, if $\hat{\Lambda} = \Lambda, \hat{\mu} = \mu, \hat{p} = p$ and $F_{contact} = F_{sensor}$ (perfect estimation) then the closed-loop system can be shown to be equivalent to the double integrator: $\ddot{x} = u = \begin{bmatrix} u_{motion} & u_{active-force} \end{bmatrix}^T$. As a result, it can be shown that the system can achieve asymptotic tracking by choosing appropriate PD gains in (11-12) [1].

For redundant manipulators, the dynamically consistency generalized inverse of the Jacobian matrix (7) can be used to dynamically decouple the operational space and null space dynamics [1, 11, 12]:

The null-space control is then formulated as follows:

$$\tau = J^T F + \left(I - J^T \bar{J}^T \right) \tau_{null} \qquad (13)$$

For simplicity, throughout this paper, we will adopt a simple null-space control as follows:

$$\tau_{null} = -K_{nD}\dot{q} - \nabla V_0 \qquad (14)$$

$$V_0 = \frac{1}{2}(q - q_{rest})K_{nP}(q - q_{rest}) \qquad (15)$$

where q_{rest} is some preferred joint configuration.

In OSC, the joint friction is normally compensated at the joint level:

$$\tau = J^T F + \left(I - J^T \bar{J}^T \right) \tau_{null} + \hat{\tau}_{friction} \qquad (16)$$

As a result, any local remaining un-model/non-linear effects at joint-space D_τ will only be compensated at the task-level through the kinematic chains as in (6). It is easily to see from (6) that the bounded disturbance D_τ in joint space can become unbounded disturbance D_F in task space when the manipulator is near singular configuration. In other words, the unmodeled dynamics will have a significant contribution to the task space control performance. This effect becomes worse in the presence of joint redundancy since all the disturbances from the n joints, with $n > 6$, are combined into task space. As a result, performance of the conventional OSC is heavily dependent on the accuracy of the system dynamic model. This observation is also confirmed in [2] where the performance of the force-based OSC is worse compared with other OSCs (Figure 3-5 in [2]).

Since it is difficult to obtain a perfect dynamic model, in this paper, we adopt another approach where inner high speed joint velocity control loops are used to suppress the unmodeled dynamics of the system as well as the friction effects at each joint. Consequently, the task space control performance is significantly improved as illustrated in the next section.

B. New implementation of the force-based operational space control

Before presenting the new approach, let us review some of the key features of the above force-based OSC (this is also the reason why we choose to adopt this OSC methods among others, please refer to [2] for a comprehensive review):

(i) The task space control performance is supposed to be isotropic for any working condition i.e. high-speed and low-speed tasks. This is because the dynamic model is considered (9-10) and (16).

(ii) The task space (range space) and null space are dynamically decoupled. This implies that the null space can be fully utilized to fulfill the sub tasks (such as obstacle avoidance or avoiding singularity) without affecting the task space performance.

(iii) The OSC is a force-based controller (8), thus, this control scheme provides a natural and physically intuitive framework for interaction tasks in the operational space [13].

As earlier mentioned, the above OSC, which works perfectly in the simulation environment, is sensitive to the modeling errors. Thus, in order to retain the advantages of force-based OSC while rejecting the effects of modeling uncertainties on the system performance, the following two layered hierarchical control scheme is proposed as follows:

- **Inner loop:** a computed torque controller is used to control the joint velocity of the robots. The use of the dynamic model (included viscous and Coulomb friction) here will enhance the performance as in [3]. The input of this controller is the reference joint velocities, the controller can be stated as:

$$\tau_{JSC} = \hat{A}u + \hat{C} + \hat{G} + \hat{\tau}_{Fric} + J^T F_{sensor} \qquad (18)$$

$$u = \ddot{q}_{desired} + K_P(\dot{q}_{desired} - \dot{q}) + K_I \int (\dot{q}_{desired} - \dot{q})dt \qquad (19)$$

- **Outer loop:** the operational space command force is computed as in (8-10). This virtual force is then transformed into joint torque τ_{OSC} using (13).

If the model is perfect (so the disturbance also equal to zero), the joint responses after Δt (s), which is the sampling period of the outer loop, can be computed by integrating the output of the joint space dynamics:

$$\ddot{q} = \hat{A}^{-1} \left(\tau_{OSC} - \hat{C} - \hat{G} - J^T F_{sensor} \right) \qquad (20)$$

$$\{\dot{q}(t + \Delta t), q(t + \Delta t)\} \triangleq \int_t^{t+\Delta t} \ddot{q}(t)dt \qquad (21)$$

with the initial condition as the current $\{\dot{q}(t), q(t)\}$.

Clearly that if the inner velocity control loop is able to bring the manipulator from the current state $\{\dot{q}(t), q(t)\}$ to $\{\dot{q}(t + \Delta t), q(t + \Delta t)\}$ after Δt

(s), the behavior of the robot will be exactly determined by the identified dynamic model: $\{\hat{A}, \hat{C}, \hat{G}\}$. In other words, the dash box in Figure 2 simulates the following dynamic system:

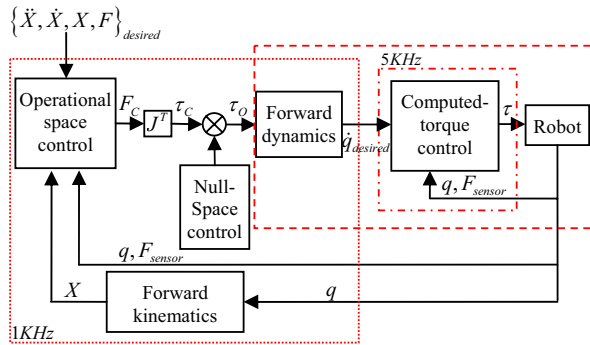$$\hat{A}(q)\ddot{q} + \hat{C}(\dot{q}, q) + \hat{g}(q) = \tau - J^T F_{sensor} \qquad (22)$$

Figure 2. The proposed two-loop controller: (dot frame): outer loop, (dot-dash frame): inner loop

Note that the assumption that the inner velocity control loop can change the system states in Δt (s) is usually violated in practice, thus, an outer loop, which is the force-based OSC, is always necessary to ensure the task space performance.

III. EXPERIMENTAL RESULTS FOR THE PA10 MANIPULATOR

In order to show the efficiency of the proposed scheme, the above controller is implemented on the Mitsubishi 7-DOF PA10 manipulator.

A. Experiment testbed

In order to achieve real-time torque control capability, the original controller of the PA10 has been replaced by our custom controller which is depicted in Figure 3a.
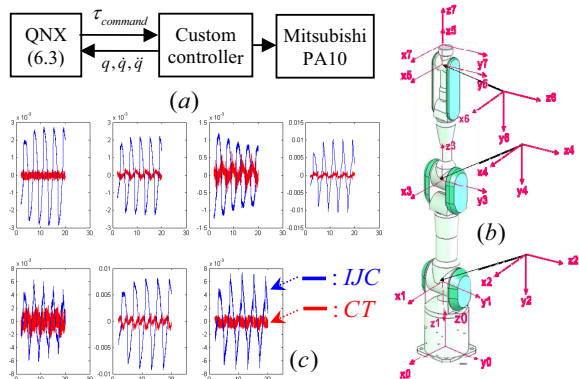

Figure 3. (a) Experiment testbed. (b) The PA10 manipulator. (c) Joint tracking errors using independent joint control scheme (IJC) and computed-torque (CT) control scheme (using the identified model).

The dynamic model of the manipulator was identified as in [3]. For advanced model-based control, it is necessary to ensure that the joint space inertial matrix A is positive definite for all configurations. This can be achieved by applying a constraint optimization technique on the obtained data during the identification experiments as suggested in [3]. In order to verify the quality of the identified parameters, a conventional computed-torque scheme was implemented. Joint tracking errors for an arbitrary trajectory are shown in Figure 3c. From Figure 3c, it can be seen that there is a significant improvement in comparison to the independent joint control scheme which verifies the quality of the identified model.

B. Conventional OSC implementation vs. the proposed implementation: task space motion control

In this experiment, the identified dynamic model is used in both schemes:

- Conventional OSC implementation: a straight forward implementation of the OSC as in Section 2A. Noting that due to the effects of model uncertainties, the OSC's motion control gains (11) were tuned to reach the performance limits using a similar approach as describe in section 6 of [2].

- The proposed OSC implementation: a two-layered hierarchical controller as illustrated in Figure 2 is used. Note that only a simple Euler method was used to integrate (21) because the integration always used the current states $\{\dot{q}(t), q(t)\}$ as an initial condition. The motion control gains (11) of the OSC in this case are fixed at $K_{mp} = 4000I, K_{md} = 120I$ for all experiments.

In order to evaluate the control performance, the end-effector of the manipulator was commanded to move 0.2 meter in the y-direction of the base frame in 2 seconds from the same initial configuration for both control schemes.
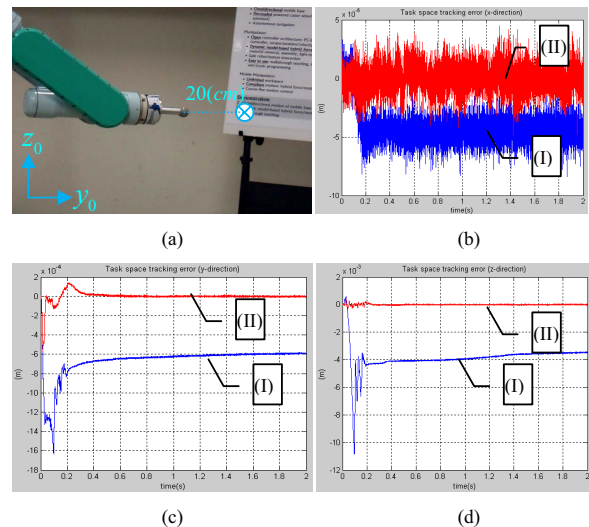

Figure 4. (a) Experiment setup. (b) Tracking error in x-direction. (c) Tracking error in y-direction. (d) Tracking error in z-direction.

The task space position tracking errors are shown in Figure 4: (I) - conventional implementation, (II) – proposed implementation. The poor performance of the conventional implementation can be explained by analyzing the friction effects at each joint. Experimental results (not shown here) indicated that joint frictions of the PA10 are significantly nonlinear due to the Stribeck effect, hysteresis effect and is found to be position and time varying. Clearly, the simple friction model (viscous and Coulumb) is not able to fully describe these effects. These effects are magnified in operational space; the performance is therefore degraded significantly in case (I). On the other hand, the proposed two-layered hierarchical controller has an inner-loop control to suppress these nonlinear effects efficiently since the control loops are closed *at the joint level*.

C. Task space motion control: low-speed vs. high-speed

The performance of the proposed control scheme is also evaluated for the high-speed and low-speed tasks. In this case, the end-effector is commanded to move in a star-like trajectory as in Figure 5a-5b. For the high-speed task, each segment is commanded to move in 1 second. For low-speed case, this value becomes 2 seconds. Position tracking errors are shown in Figure 5c-5d (noting that the control gains for both cases are the same).

(a)   (b)
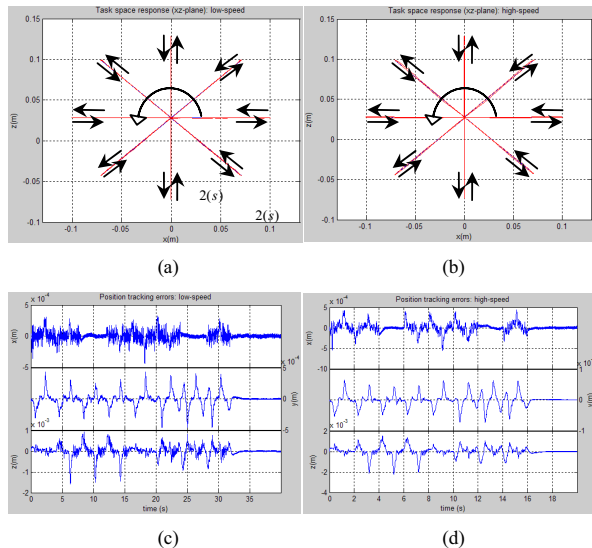

(c)   (d)

Figure 5.   (a) Low-speed task space response. (b) High-speed task space response. (c) Low-speed position tracking errors. (d) High-speed position tracking errors

From the above figures, it can be seen that even at a sufficiently high-speed (0.1 ms^{-1}), the tracking errors are still around 0.1 mm which verifies the effectiveness of the dynamic model compensation.

To demonstrate the effects of null space on the task space performance, the end-effector is commanded to hold at the current position and orientation. Sinusoidal trajectories were applied to joint 1 as in (13-15). The task space position tracking errors is presented in Figure 6.
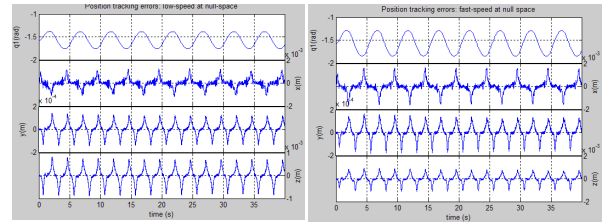

Figure 6.   Position tracking errors for different null space trajectories (from top to bottom: q_1, x_{error}, y_{error}, z_{error})

Figure 6 indicates that the task space tracking errors for two different null space trajectories of joint 1 are about the same order of magnitude. This implies that the null space and task space (range space) are nearly decoupled (section 2B – (b)). It is worth noting that theoretically, the null space and the task space should be totally decoupled. However, due to the inaccuracy of the kinematic model and unmodeled dynamics, one should expect to see a slightly coupling between them. However, these effects are minimized under the force-based OSC as discussed previously.

D. Hybrid motion and force control

The motion and force control capability of the proposed control scheme was evaluated using two experiments as follows:

Force regulation: as mentioned before, regulating the contact force is really a challenge for the conventional implementation of the OSC in the presence of model uncertainties. In fact, because of the unmodeled dynamics, it is nearly impossible to maintain 1N contact force at the end-effector. However, as shown in Figure 7, the proposed controller is able to maintain a light (1N) as well as a slightly heavy (10N) contact force without any retuning of force gains. Note that in this experiment, only x-direction (base frame) is force controlled. Other axes (y, z and orientation) are motion controlled.

(a)   (b)
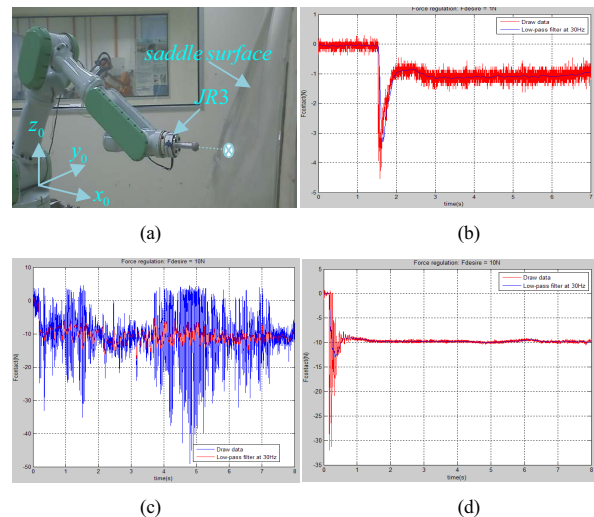

(c)   (d)

Figure 7.   (a) Experiment setup. (b) Desired force = 1N - Proposed scheme. (c) Desired force = 10N - conventional implementation. (d) Desired force = 10N - Proposed scheme.

Notice that the chattering in Figure 7c is mainly due to the interaction between the remaining un-compensated frictions at each joint and the contact force as also observed in [14]. Because of the inner velocity loop at each joint, these effects have been removed for the proposed scheme. Noting that a similar experiment was conducted in [15] using the conventional OSC implementation. However, in order to achieve a similar performance as in Figure 7d, the OSC needed to run at higher sampling rate (8KHz). Moreover, practically, it is nearly impossible to maintain the contact force at 1N using the conventional OSC even if the sampling rate is increased to 8KHz as discussed above.

Motion and force control: in order to have a better benchmark of the force control capability, the proposed control scheme has been compared to the commercial force control solution from PushCorp. Because Pushcorp's compliance module only has the capability of regulating the force in one axis, the compliance module (AFD1100) was attached to the end-effector of the ABB robot (IRB4400) as depicted in Figure 9b. The ABB robot is then commanded to move in x-direction while the PushCorp compliance module regulated the contact force in the y-direction as illustrated in Figure 8.
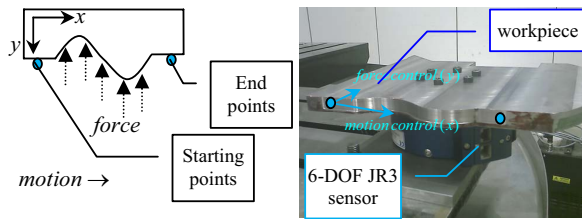

Figure 8. Experiment setup.

In this experiment, the task is to move the end-effector from the starting point to the end point while maintaining the contact force to be 20N. In order to have a fair comparison, an independent JR3 sensor has been installed at the bottom of the workpiece. The measured forces from sensor for the proposed force control using PA10 and the Pushcorp's compliance module are presented in Figure 9a. As the result shows, the force tracking error of the Pushcorp's module and the PA10 force control are are similar. However, the PA10 controller has to control a 7-DOF system while the PushCorp device is only concerned with the force control of a single axis. This observation implied that the proposed controller is able to perform as good as the 1-DOF system and still maintains the flexibility of the 7-DOF system.
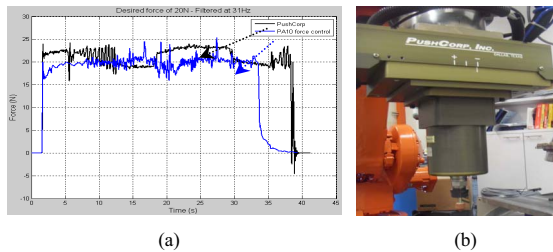

(a)   (b)

Figure 9. (a) Comparion on one axis force control (desired force = 20N). (b) ABB and Pushcorp compliance module.

IV. CONCLUSION

In this paper, we have presented a two-layered hierarchical control structure with an inner joint velocity control loop and an outer force-based OSC loop. Due to the closing of the inner loops at the joint level, joint disturbance are efficiently rejected. The proposed control scheme has been intensively evaluated using the PA10 manipulator. Experimental results have shown that the proposed controller performed better than the conventional force-based OSC. The proposed controller has been compared with a commercial force control module from PushCorp. The experimental results show that the proposed controller is able to achieve similar performance even though the control problem is significantly more complex. Future work will be conducted to analyze the stability of the proposed controller.

REFERENCES

1. Khatib, O., *A unified approach for motion and force control of robot manipulators: the operational space formulation.* IEEE Journal of Robotics and Automation, 1987. **RA-3**(1): p. 43-53.
2. Nakanishi, J., et al., *Operational space control: A theoretical and empirical comparison.* International Journal of Robotics Research, 2008. **27**(6): p. 737-757.
3. Ngoc Dung, V. and J. Marcelo H. Ang, *Dynamic Model Identification For Industrial Manipulator Subject To Advanced Model Based Control*, in *4th HNICEM*. 2008: Manila, Philippines.
4. Ngoc Dung, V. and J. Marcelo H. Ang, *Improved dynamic identification of robotic manipulators in the linear region of dynamic friction - to appear*, in *The 9th International IFAC SYROCO* 2009.
5. Olsson, H., et al., *Friction models and friction compensation.* European Journal of Control, 1998. **4**(3): p. 176-95.
6. Canudas De Wit, C. and P. Lischinsky, *Adaptive friction compensation with partially known dynamic friction model. Journal of Adaptive control*, 1997. **11**(1): p. 65-80.
7. Hensen, R.H.A., *Controlled Mechanical Systems with Friction*. 2002, University Press Facilities. p. 186.
8. Kelly, R. and J. Moreno, *Manipulator motion control in operational space using joint velocity inner loops.* Automatica, 2005. **41**(8): p. 1423.
9. Camarillo, K., et al., *Stability analysis of the operational space control for industrial robots using their own joint velocity PI controllers.* Robotica, 2008. **26**(6): p. 729-738.
10. Oetomo, D. and M.H. Ang, Jr., *Singularity robust algorithm in serial manipulators.* Robotics and Computer-Integrated Manufacturing, 2009. **25**(1): p. 122-34.
11. Featherstone, B. and O. Khatib, *Load independence of the dynamically consistent inverse of the Jacobian matrix.* International Journal of Robotics Research, 1997. **16**(2): p. 168-70.
12. Bruyninckx, H. and O. Khatib. *Gauss' principle and the dynamics of redundant and constrained manipulators*. ICRA, 2000.
13. Sentis, L. and O. Khatib, *Synthesis of whole-body behaviors through hierarchical control of behavioral primitives.* International Journal of Humanoid Robotics, 2005. **2**(4): p. 505-518.
14. Townsend, W.T. and J.K. Salisbury, Jr. *The effect of Coulomb friction and stiction on force control*. in *ICRA*, 1987. Washington, DC, USA.
15. Tao Ming, L., et al. *Unified force and motion control using an open system real-time architecture on a 7 DOF PA-10 robot*. in *Advanced Intelligent Mechatronics. Proceedings, 2005 IEEE/ASME International Conference on*. 2005.